Featured Article

In vitro degradation of β-amyloid fibrils by microbial keratinase

Debananda S. Ningthoujam[a],[**],[1], Saikat Mukherjee[a],[*],[1], Laishram Jaya Devi[a],
Elangbam Shanta Singh[a], Keishing Tamreihao[a], Rakhi Khunjamayum[a], Sumita Banerjee[b],
Debashis Mukhopadhyay[c]

[a]Department of Biochemistry, Advanced Level State Biotech Hub, Microbial Biotechnology Research Laboratory, Manipur University, Imphal, Manipur, India
[b]Department of Oral Pathology, Dental College, Regional Institute of Medical Sciences, Imphal, Manipur, India
[c]Biophysics and Structural Genomics Division, Saha Institute of Nuclear Physics, Kolkata, West Bengal, India

Abstract

Introduction: Amyloid fibrils are misfolded, protease-resistant forms of normal proteins. They are infectious such as prions or noninfectious such as β-amyloid (Aβ) fibrils causing Alzheimer's disease (AD). Prions and amyloids are structurally similar, possessing cross β-pleated sheet-like structures. As microbial keratinase could degrade prions, we tested keratinase activity on Aβ fibrils.

Methods: Lysozyme treated with urea generates Aβ fibrils demonstrated by immunoblotting with anti-Aβ antibody, high-performance liquid chromatography, and Congo red absorption spectroscopy. Two keratinases, Ker1 and Ker2, were purified from an actinomycete Amycolatopsis sp. MBRL 40 and incubated with Aβ fibrils.

Results: Soluble Ker1 and Ker1 reconstituted on neutral/cationic liposomes degraded Aβ fibrils efficiently. Ker 2 was less potent.

Discussion: Drugs that target AD inhibit acetylcholinesterase or formation of Aβ fibrils and downstream effects. These drugs have side effects and do not benefit globally in cognition. Keratinases are novel molecules for drug development against AD.

© 2019 The Authors. Published by Elsevier Inc. on behalf of the Alzheimer's Association. This is an open access article under the CC BY-NC-ND license (http://creativecommons.org/licenses/by-nc-nd/4.0/).

Keywords: Actinomycete; Keratinase; β-amyloid fibrils; Ker 1; In vitro degradation

1. Background

1.1. Amyloid fibrils

Amyloids are misfolded forms of normal proteins which interact erroneously and generate insoluble aggregates or proteolysis-resistant fibrils. More than 20 plasma proteins form amyloids and its deposition cause various diseases. These proteins differ in primary structure; however, after conversion to an amyloidogenic form, they possess unique β-sheet conformation (cross β-sheet) which makes them insoluble, fibrillar, and resistant to protease [1–5]. Structural models of amyloid have been developed by electron microscopy, X-ray diffraction, solid state nuclear magnetic resonance, Congo red absorption spectroscopy, circularichroism spectroscopy, and electron paramagnetic resonance [6–8]. Dyes such as Congo red and thioflavin T are used for monitoring the kinetics of amyloid aggregation [9].

Systemic diseases such as immunoglobulin light-chain amyloidosis, hereditary lysozyme amyloidosis, diabetes type II, and localized neurodegenerative diseases such as Alzheimer's disease (AD), Huntington's disease, Parkinson's disease, motor neuron disease, prion diseases, and forms of dementias are caused by deposition of amyloid fibrils in particular tissue concerned [9–13].

Conflicts of interests: None declared.

[1]Both authors contributed equally to the study.

*Corresponding author. Tel.: +918787490855; Fax: +913852435145.

**Corresponding author. Tel.: +919862027271; Fax: +913852435145.

E-mail address: mukherjeesaikat333@gmail.com (S.M.), debananda.ningthoujam@gmail.com (D.S.N.)

1.2. Alzheimer's disease

Amyloid fibrils deposited in brains cause AD. They are abnormal clumps of toxic fragments (39–43 aa peptide), known as amyloid-β peptide (Aβ). The peptide is found in the extracellular space between nerve cells blocking synaptic transmission leading to degeneration of neurons [14].

1.3. Role of keratinases in degrading prions

Some amyloids such as prions (Mad cow disease or Kuru) are infectious. A normal cellular form of α-helical prion protein (PrPC) gets converted into an insoluble, protease-resistant, cross β sheet abnormal form (PrPSc) that resists common proteases [15,16].

Different physical and chemical methods had been used to treat PrPSc [17–19]; however, these methods had limitations. An alternate approach is the enzymatic degradation of prions using microbial keratinases. Microbial keratinases are proteases that effectively degrade sturdy proteins such as keratin [20]. Keratinases are produced by several microbial species including fungi [21,22], actinomycetes [23] especially genus *Streptomyces* [24,25], *Bacillus* [26,27], and archaea [28]. A keratinase purified from *Bacillus licheniformis* PWD-1 degraded prions efficiently [29]. Thereafter, more prion-degrading keratinases were identified [30,31]. Recently, genetically modified proteases have been developed that can degrade prions efficiently [32,33].

1.4. Keratinases and Aβ fibrils

Aβ fibrils and prions possess cross β-pleated sheet-like structures. We investigated the activity of keratinases on Aβ fibrils *in vitro*. Earlier, we isolated chicken feather–degrading actinomycetes, *Amycolatopsis* sp. MBRL 40, in our laboratory from soil samples collected from a limestone habitat [34]. We purified two keratinases, Ker1 and Ker2, from this strain and tested on Aβ fibrils.

Amyloids may also not be associated with any diseases [35–38]. An excellent example is amyloid fibrils formed from hen egg white lysozyme (HEWL). HEWL is a model system to study Aβ fibril formation. HEWL forms Aβ fibrils in the presence of ethanol, heat, acid, or guanidine hydrochloride [39–42]. We generated Aβ fibrils of lysozyme *in vitro* using urea and demonstrated formation of these fibrils by Congo red absorption spectroscopy, immunoblotting with anti-Aβ antibody and high-performance liquid chromatography. Aβ fibrils of lysozyme were completely digested by soluble Ker1 as well as Ker1 reconstituted on neutral and cationic liposomes. Soluble or reconstituted Ker2 partially digested Aβ fibrils of lysozyme after 24 hrs of incubation.

2. Methodology

The reagents were purchased from HiMedia or Sigma-Aldrich unless otherwise mentioned.

2.1. Preparation of inoculum

Amycolatopsis sp. MBRL 40 was grown as described in the study by Ningthoujam et al [34].

2.2. Production of keratinase

Keratinase production was carried out in feather basal medium (FBM) in the presence of chicken feather as described in the study by Ningthoujam et al [34].

2.3. Purification of keratinases

The FBM culture broth was centrifuged (10,000 rpm, 15 mins, 4°C). The pellet was discarded, and the supernatant containing the crude enzyme was saturated with 80% solid $(NH_4)_2SO_4$ and precipitated overnight at 4°C. The precipitate was recovered by centrifugation (5000g, 15 mins, 4oC). The pellet was dissolved in 5 ml of 50 mM phosphate buffer, pH 7.0, and dialyzed for 8 hrs against 1 liter of 50 mM phosphate buffer, pH 7.0, at 4°C with three changes of buffer. The dialyzed enzyme was subjected to purification using Q Sepharose Fast Flow, swollen, 45-165 μm (1 ml of dialyzed enzyme fractions was loaded onto the Q Sepharose Fast Flow column [5 × 30 cm] previously equilibrated with 50 mM phosphate buffer [pH 7.0]). After clearing the unbound fraction in 50 mM phosphate buffer, bound fractions were eluted using 50 mM phosphate buffer containing linear concentration gradients of NaCl (0.25 M, 0.5 M, 1 M, and 2 M). Fractions of 1.0 ml each were collected at a flow rate of 0.2 ml/min. The protein concentration of each fraction was determined at 280 nm using a UV-Vis spectrophotometer (Beckman Coulter). Eluants 0.5 M NaCl and 1 M NaCl were found to be active. The fractions were further dialyzed for 5 hrs in 50 mM phosphate buffer without NaCl at 4°C. The final dialyzed fractions of 1 M and 0.5 M fractions were named as Ker1 and Ker2, respectively. The protein contents of the purified keratinases were estimated by the Lowry method using Bovine Serum Albumin as standard.

2.4. Keratinase activity assay

The activities of purified Ker1/Ker2 or total crude keratinase were determined using substrates such as Keratin Azure, chicken feather, and soluble keratin [43–45].

2.5. Assay of protease activity

Proteolytic activities of Ker1, Ker2, and total crude keratinase were measured using casein as the substrate. One milliliter of 1% casein and 1 ml of Ker1 or Ker 2 or 1 ml of appropriately diluted crude keratinase were mixed

with 3 ml of 50 mM phosphate buffer pH 7.0 and incubated at 40°C for 20 minutes. The reaction was stopped by adding 1 ml of 5% trichloroacetic acid and incubated at room temperature for 30 mins, followed by centrifugation (7000 rpm, 5 mins). The proteolytic products in supernatants were determined by recording the absorbance of the supernatant at 280 nm. Standards were prepared using 10-100 µg of tyrosine, and one unit of protease is defined as the amount of enzyme required to release 1 µg of tyrosine per minute under standard assay condition.

2.6. Formation of Aβ fibrils of lysozyme

HEWL (1 mg/ml) was incubated with 8 M urea (48 hrs, 55°C) in 1 ml of 50 mM phosphate buffer (pH 7.0) to enable formation of Aβ fibrils. The fibrils settled as white fibrous precipitates at the bottom of microcentrifuge tubes.

2.7. Treatment of Aβ fibrils with Ker1/Ker2

Fibrous precipitates of Aβ fibrils were suspended by vortexing in 50 mM phosphate buffer (pH 7.0) and incubated with purified Ker1 or Ker 2 at various concentrations (50 µg/ml, 100 µg/ml, 125 µg/ml, 250 µg/ml, 500 µg/ml) for various time intervals (0 hr, 3 hrs, 6 hrs, 12 hrs, 24 hrs) at 40°C.

2.8. Sodium dodecyl sulfate polyacrylamide gel electrophoresis and immunoblotting

Purified Ker1, Ker2, or Aβ fibrils were fractionated using Bio-Rad Mini-PROTEAN sodium dodecyl sulfate polyacrylamide gel electrophoresis (SDS-PAGE) electrophoresis system. The molecular weights of Ker1 and Ker2 were estimated by comparing the relative mobility of proteins with protein markers of different molecular sizes (97.4 – 20.1 kDa; Genei, Bangalore, Karnataka, India). For immunoblotting, the gels were blotted onto nitrocellulose membrane (GE Healthcare). Membrane blocking was performed by immersing the membrane in blocking buffer (20 mM Tris-HCl, pH 7.5, 150 mM NaCl, 5% bovine serum albumin, 0.02% sodium azide, 0.1% Tween 20) for 1 hr at room temperature. The blots were incubated with blocking buffer containing anti-mouse Aβ antibody (1:500 dilution) for 1 hr at 4°C. After incubation with the primary antibody, the blots were washed thrice for 10 mins with blocking buffer and incubated with goat anti-mouse alkaline phosphatase conjugated secondary antibody (1:10,000) for 1 hr at room temperature. After washing the blots thrice for 10 mins, color development was carried out in 20-ml color development buffer containing 100 mM Tris-HCl (pH 9.5), 5 mM MgCl2, 100 mM NaCl containing nitro-blue tetrazolium chloride (2 mg/ml) and 5-bromo, 4-chloro, 3-indolyl phosphate (1 mg/ml).

2.9. Preparation of Ker1-loaded proteoliposomes

All lipids were purchased from Avanti Lipids, Alabaster, AL, USA. For neutral liposome preparation, phosphatidylcholine and phosphatidylethanolamine were used. For cationic liposomes, cationic lipids 1,2 dioleoyl-sn-glycerol-3-phosphoethanolamine (DOPE) and 1,2–dioleoyl-3-trimethyl amino propane (chloride) salt (DOTAP) were used. The lipids were dissolved separately in 100% ethanol at 10 mg/ml. For empty neutral liposome preparation, 10 mg equivalent of phosphatidylcholine was mixed with 50-mg equivalent of phosphatidylethanolamine in a glass vial. A thin lipid film appeared on the walls of the glass vial while rotating the glass vial and evaporating the solvent in air. The lipid film was rehydrated by addition of 5 ml of 50 mM phosphate buffer (pH 7.0). The lipid suspension was disrupted by several freeze-thaw cycles and extruded through filters with a 0.2-µm pore size to obtain a homogenous suspension of unilamellar lipid vesicles. Liposomes were further purified by ultracentrifugation (Beckman Coulter Model No: Optima L-90K) for 2 hrs at 1,00,000g (30,000 rpm) using Type 45 Ti rotor. For empty cationic liposome preparation, 10 mg equivalent of DOPE was mixed with 50 mg equivalent of DOTAP, and a similar methodology of neutral liposome preparation was followed. For protein reconstitution, 1 ml of liposome suspensions (neutral or cationic) were destabilized with 0.05% Tween 20, and 250 µg of solubilized Ker1 was added. The protein-liposome mixture was incubated for 2 hrs at 4°C. Ker1-reconstituted liposomes were dialyzed overnight against 1 liter of 50 mM phosphate buffer (pH 7.0), and protein-loaded liposomes were further purified by ultracentrifugation for 2 hrs at 1,00,000g (30,000 rpm) using Type 45 Ti rotor. Formation of Ker1-loaded proteoliposomes was confirmed by disrupting the proteoliposomes with 1% SDS and monitoring the increase in absorbance of the supernatant at 280 nm due to release of Ker1 from the liposomes into supernatant.

2.10. High-Performance Liquid Chromatography

Lysozyme, Aβ fibrils, and Ker1-treated Aβ fibrils were analyzed in a Agilent 1600 Infinity Series HPLC System (C18 column, 100% water solvent, flow rate: 1.0 ml/min, 50 mM phosphate buffer [pH 7.0]). The retention time (tR) of the peaks was recorded.

2.11. Congo red absorption spectroscopy

Congo red was added at a final concentration of 18 µM to microcentrifuge tubes containing 50 mM phosphate buffer (pH 7.0) that included soluble lysozyme, fibrous precipitates of Aβ fibrils, or Aβ fibrils solubilized or partially solubilized with Ker1/Ker2. The contents were mixed thoroughly in a vortex, and the tubes were incubated for 15 mins at room temperature. The spectrum of Congo red was monitored from 400 nm to 700 nm in a UV-Vis spectrophotometer (Beckman Coulter Model no: DU730).
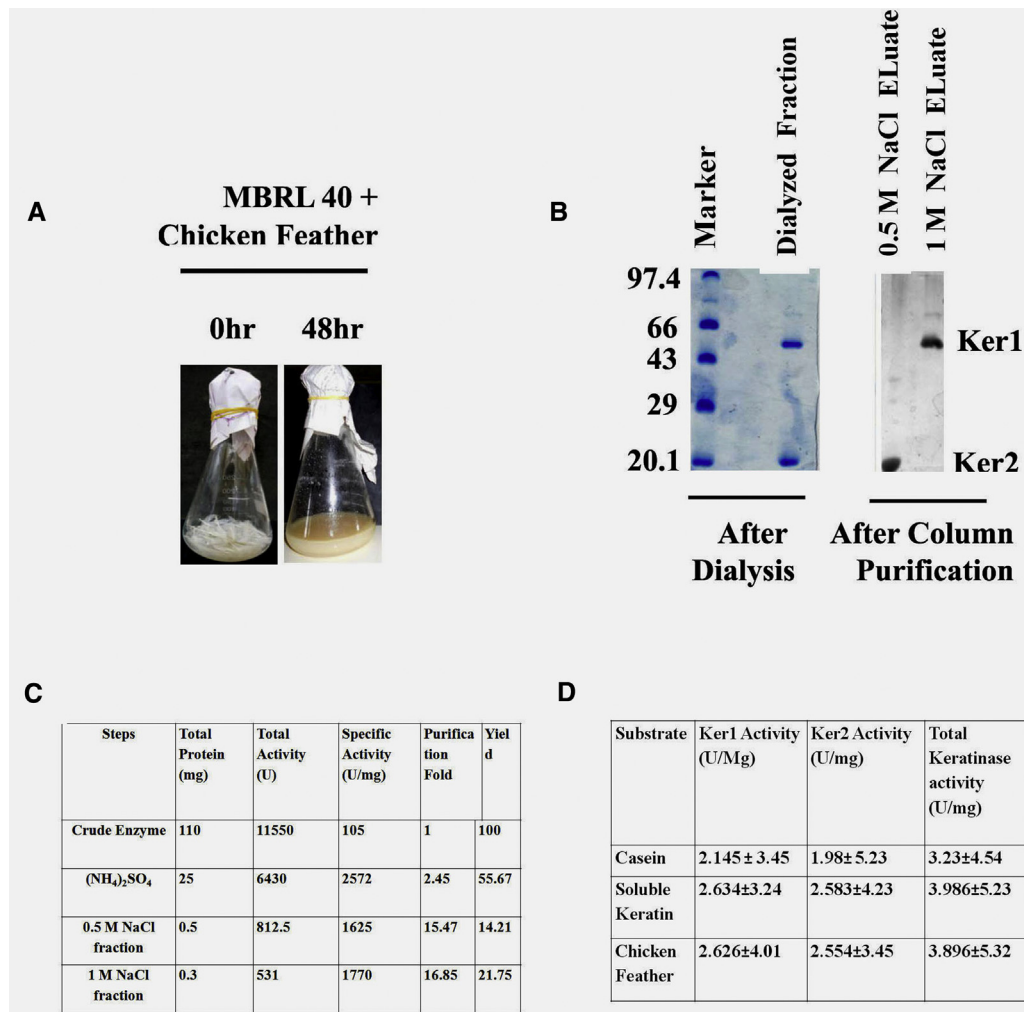
Fig. 1. Production, purification, and activity assay of Ker 1 and Ker 2 keratinase. (A) Degradation of chicken feather by *Amycolatopsis sp.* MBRL 40 in feather basal medium (FBM) at 0 hr and 48 hr after incubation. (B) Purification of Ker1 and Ker2 by dialysis (left panel) and Q Sepharose column chromatography using 0.5 M NaCl as eluant (Ker 2, 20.1 kDa) and 1 M NaCl as eluant (Ker1, 50.1 kDa) (right panel). The molecular markers are denoted as 97.4 kDa, 66 kDa, 43 kDa, 29 kDa, and 20.1 kDa. (C) Sequential steps of purification of Ker1 (1 M NaCl eluent fraction) and Ker2 (0.5 M NaCl eluent fraction) starting from the crude enzyme. (D) Activity assay of purified Ker1 and Ker2 using casein, soluble keratin, and chicken feather as substrates.

3. Results

3.1. Production, purification, and activity of Ker1 and Ker2 keratinases

Amycolatopsis sp. MBRL 40 degraded insoluble chicken feathers completely after 48 hrs incubation at 40°C, resulting in clearance of FBM when compared with 0 hr of incubation (Fig. 1A). Fractionation of the dialyzed broth on a Q Sepharose column resulted in elution of two major fractions at 0.5 M and 1 M NaCl. The dialyzed fraction as well as 0.5 M and 1 M NaCl fractions were analyzed by SDS-PAGE. Although dialyzed fraction showed two protein bands (20.1 and 50.1 kDa) (Fig. 1B, left panel), 0.5 M and 1 M NaCl fractions showed single protein band of molecular weights 20.1 kDa and 50.1 kDa, respectively (Fig. 1B, right panel). NaCl fractions of 1 M and 0.5 M were named as Ker1 and Ker2, respectively.

The specific activity of each fraction was determined using keratin azure as substrate. The crude enzyme showed total activity of 11,550 U and specific activity of 105U/mg (Fig. 1C). The enzyme in the dialyzed fraction had total activity of 6430 U, specific activity of 2572 U/mg, purification fold of 2.45, and yield of 55.67% when compared with the crude enzyme. Q Sepharose column chromatography resulted in increase in specific enzyme activity in both 0.5 M and 1M NaCl eluted fractions. The 0.5 M NaCl fraction showed total activity of 812.5 U and specific activity of 1625 U/mg resulting in purification fold of 15.47 and yield of 14.21%, as compared with crude enzyme. We observed highest specific activity in 1 M NaCl fraction with keratin azure as substrate. Total activity of 531 U was showed by 1M NaCl fraction, and specific activity was 1770 U/mg with purification fold of 16.85 and yield of 21.75%, as compared with crude (Fig. 1C)
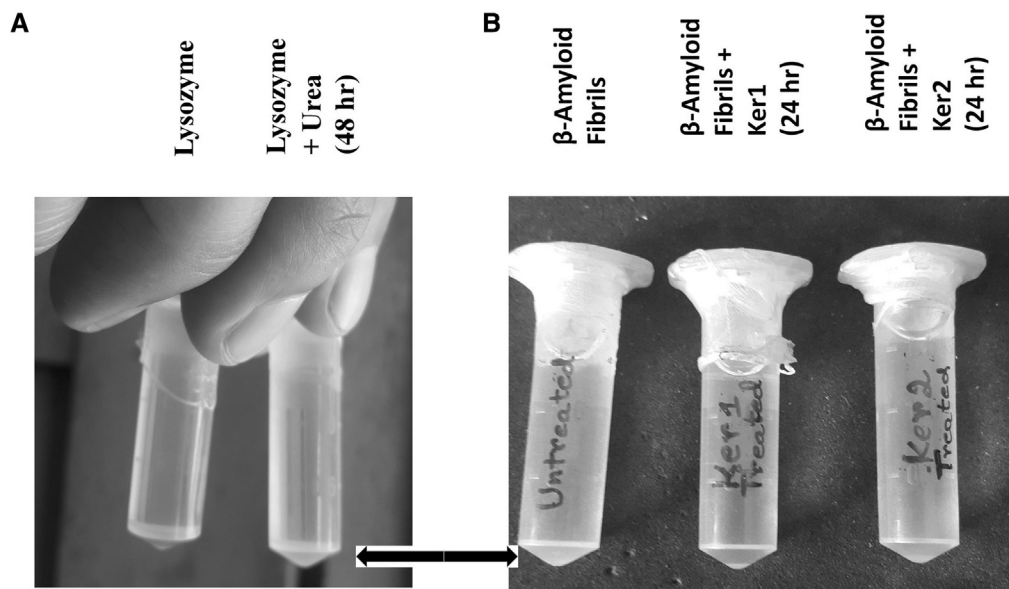
Fig. 2. Activity of Ker1 and Ker2 on β-amyloid (Aβ) fibrils of lysozyme. (A) Tubes showing lysozyme alone (left) and Aβ fibrils of lysozyme (right), i.e., lysozyme incubated with urea for 48 hr. (B) Treatment of Aβ fibrils with Ker1 and Ker2. Aβ fibrils untreated (left), Aβ fibrils treated with Ker1 for 24 hr (middle), and Aβ fibrils treated with Ker2 for 24 hr (right). White, fibrous precipitates of amyloid fibrils at the bottom of the tubes are denoted by solid arrows.

Both Ker1 and Ker2 degraded casein, chicken feather, and soluble keratin. Ker1 was more potent than Ker2. Ker1 had better activity on soluble keratin (2.634 U/mg) and chicken feather (2.626 U/mg) than on casein (2.145 U/mg). Similar findings were observed for Ker2 as well (Fig 1D). Both Ker1 and Ker2 were found to be keratinolytic proteases. Their activities were found to be inhibited by ethylenediaminetetraacetic acid and phenylmethylsulfonyl fluoride (data not shown), confirming the enzymes are metal-activated serine proteases.

3.2. Preparation of Aβ fibrils of lysozyme

Lysozyme, in the presence of urea, formed white, fibrous precipitates at the bottom of the microcentrifuge tubes (Fig. 2A). The precipitate, after fractionation by SDS-PAGE and immunoblotting with anti-Aβ antibody, gave positive signal, confirming formation of Aβ fibrils. However, untreated lysozyme gave no signal (Fig. 3A). To test the kinetics of Aβ fibril formation, lysozyme was treated with urea at different time points and analyzed on HPLC. Lysozyme without urea showed a peak at a retention time (tR) of 1.39 min (Fig. 3A). However, after 24 hrs of incubation, lysozyme formed three peaks with tR 1.071 min, 1.216 min, and 1.342 min (Fig. 3B), and after 48 hrs, there was a single peak at tR 1.051 min (Fig. 3C). These evidences suggest formation of amyloid fibrils of lysozyme which involves generation of various heterogeneous intermediary molecules (Fig. 3B). The peak having tR of 1.342 min is lysozyme itself, and the other peaks are the intermediary molecules. All molecules of lysozyme were finally converted to homologous Aβ fibrils after 48 hrs of incubation as represented by a sharp peak at

tR 1.05 min (Fig. 3C). Aβ fibrils are known to bind Congo red, a sodium salt of benzidinediazobis (1-napthylamine-4 sulphonic acid). Aβ aggregates stained with Congo red appear orange in white, polarized light, and apple green if placed between cross-polarizers, and binding of Congo red to amyloid fibrils results in a blue shift in the absorption spectra [46]. We analyzed the differences in the spectrum of Congo red in lysozyme solution alone and after binding with Aβ fibrils using Congo red absorption spectroscopy. Lysozyme showed a peak with λ_{max} at 522 nm and an optical density of 0.123 (Fig 5A). However, Aβ fibrils of lysozyme at 48 hrs time point showed a hyperchromic (optical density = 0.336) and a blue shift (λ_{max} = 500 nm) (Fig. 5B).

3.3. Activity of soluble Ker1 and Ker2 on Aβ fibrils

Aβ fibrils treated with Ker1 (125 μg/ml) for 24 hrs at 40°C resulted in solubilization of the white fibrous precipitate formed earlier at the bottom of the tubes (Fig. 2B). The Ker1-treated Aβ fibrils were fractionated on SDS-PAGE, followed by immunoblotting with anti-Aβ antibody. Ker1-treated amyloid fibrils produced no signal in immunoblot (Fig. 3B, lane 3), whereas untreated amyloid fibrils showed a positive signal (Fig. 3B, lane 2) confirming complete digestion of amyloid fibrils by Ker1 after 24 hrs of incubation. We had similar observations in HPLC as well. After treatment with Ker1, Aβ fibrils tend to revert to a previous unaggregated state as reflected by a change in retention time of the peak (tR = 1.268 min) (Fig. 4D). To get insights into the mechanism how Ker1 degrades Aβ fibrils, we carried out pretreatment by incubating lysozyme with Ker1 for 30 min at 4°C and then incubating the pretreated lysozyme with 8M urea for 48 hr. Immunoblotting
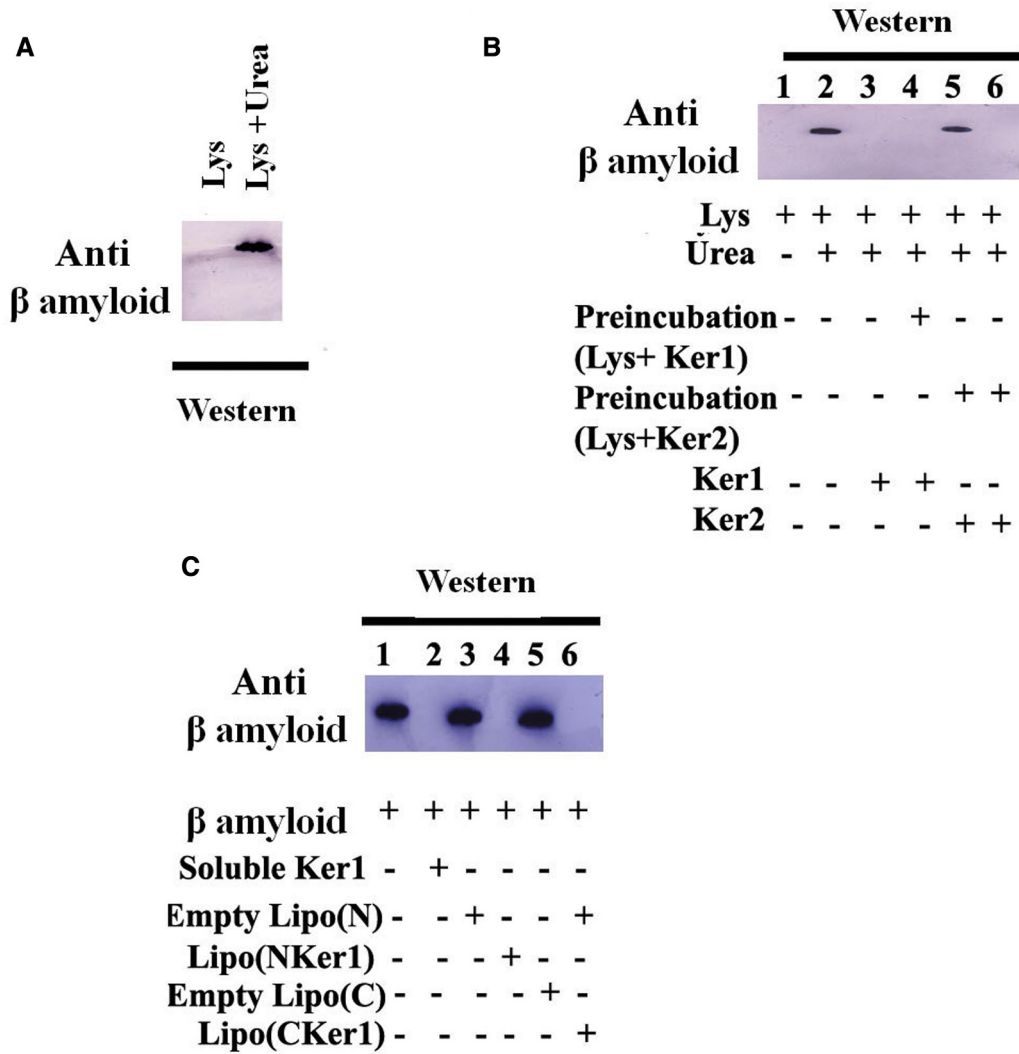
Fig. 3. Activity of Ker1 and Ker2 on β-amyloid (Aβ) fibrils revealed by immunoblotting with anti Aβ antibody. (A) Immunoblots of lysozyme alone (left panel) and lysozyme with urea-forming Aβ fibrils (right panel). (B) Complete and partial digestion of Aβ fibrils by soluble Ker1 and Ker2, respectively. Lane 1: lysozyme alone; lane 2: lysozyme and urea-forming Aβ fibrils; lane 3: Aβ fibrils treated with Ker1 for 24 hr; lane 4: lysozyme preincubated with Ker1; lane 5: Aβ fibrils treated with Ker for 24 hr; lane 6: lysozyme preincubated with Ker2. (C) Complete degradation of Aβ fibrils by liposome reconstituted with Ker1. Lane 1: input Aβ fibrils; lane 2: Aβ fibrils treated with soluble Ker1; lane 3: Aβ fibrils treated with empty neutral liposome; lane 4: Aβ fibrils treated with Ker1-reconstituted neutral liposome; lane 5: Aβ fibrils treated with empty cationic liposome; lane 6: Aβ fibrils treated with Ker1-reconstituted cationic liposome.

with anti-Aβ antibody generated no signal (Fig. 3B, lane 4). Possibly, Ker1 was blocking the formation of amyloid nucleus necessary for Aβ fibril formation. We found similar activity of Ker1 in Congo red absorption spectroscopy. Congo red after binding to Ker1-treated amyloid fibrils showed a red shift with absorption of 0.128 and a λ_{max} of 519 nm (Fig. 5C), indicating reversal of Aβ fibrils to an unaggregated state.

Ker2 was less potent than Ker1. It partially solubilized amyloid fibrils after 24 hrs, and measurable amounts of white, fibrous precipitate were still found at the bottom of the tubes (Fig. 2B). Effectively, Ker 2 takes 7 days to digest the fibrous precipitate completely (data not shown). In 24 hrs, Ker2 digestion occurs partially, as evidenced by immunoblotting with anti-Aβ antibody (Fig. 3B, lane 5), compared to the levels of Aβ fibrils alone (Fig. 3B, lane 2). The partial activity of Ker2 on Aβ fibrils was also demonstrated by Congo red absorption spectroscopy. Although the hyperchromicity of the spectrum reverted back to normal (optical density = 0.180), the spectrum still showed blue shift (λ_{max} = 506 nm) (Fig. 5D), when compared to the Aβ fibrils formed by lysozyme and urea (Fig. 5B). Although Ker2 is less potent than Ker1 in degrading Aβ fibrils, both enzymes possibly have same mechanism of action. We got similar observations when lysozyme was preincubated with Ker2. Although Aβ fibrils were partially digested after 24 hrs of incubation with Ker2 as revealed by immunoblot (Fig. 3B, lane 5), however,
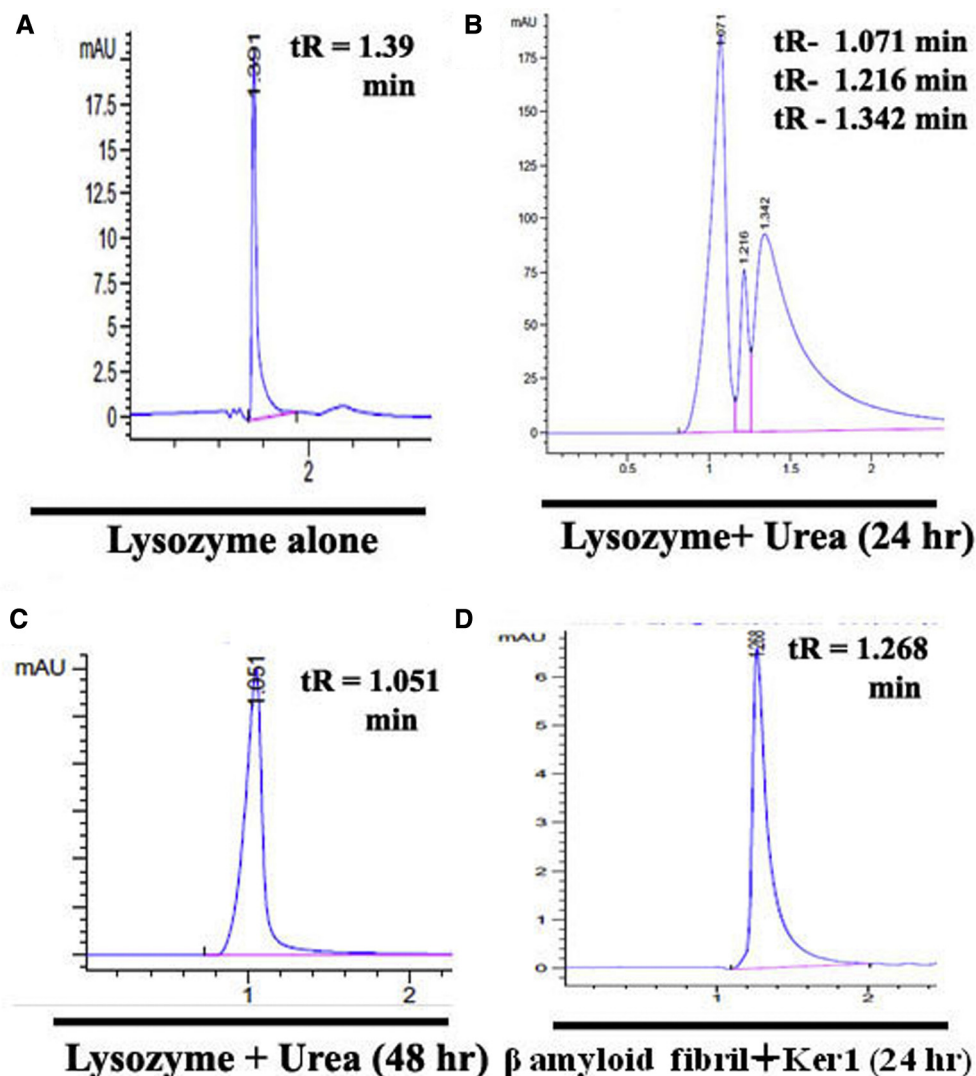
Fig. 4. Activity of Ker1 on β-amyloid (Aβ) fibrils revealed by high-performance liquid chromatography (HPLC). (A) HPLC spectrum of lysozyme alone (tR = 1.39 min). (B) HPLC spectrum of lysozyme treated with urea for 24 hr. Spectrum showing lysozyme (tR = 1.342 min) and intermediary molecules (tR = 1.216 min, 1.071 min) in the process of Aβ formation. (C) HPLC spectrum of lysozyme treated with urea for 48 hr. Spectrum showing complete conversion of lysozyme into Aβ fibrils (tR = 1.051 min). (D) HPLC spectrum of Ker1-treated Aβ fibrils. Aβ fibrils reverting back to a nonaggregated state (tR = 1.268).

preincubation of lysozyme with Ker2 blocked the formation of Aβ fibril even after incubation with 8M urea for 48 hrs (Fig. 3B, lane 6).

3.4. Reconstitution of Ker1 on neutral/cationic liposomes and activity on Aβ fibrils

We reconstituted Ker1 in liposomes and investigated whether vector formulation could degrade Aβ fibrils of lysozyme similar to soluble Ker1. Ker1 was reconstituted on both neutral phosphatidylcholine liposomes (NKer1) and cationic DOPE/DOTAP liposomes (CKer1). Both types of reconstituted liposomes were incubated separately with Aβ fibrils under same conditions as soluble Ker1. Immunoblotting with anti-Aβ antibody generated no signals with Ker1-reconstituted liposomes, indicating complete

digestion of Aβ fibrils after 24 hrs (Fig. 3C, lane 4 and lane 6). Empty neutral (N) and cationic liposomes (C) had no activity on Aβ fibrils, and positive signals were obtained when immunoblotted with anti-Aβ antibody (Fig. 3C, lane 3 and lane 5). The activities of NKer1 and CKer1 were similar to soluble Ker1 (Fig. 3C, lane 2).

4. Discussion

So far no effective pharmacotherapeutic options for prevention and treatment of AD are available. Many drugs currently being used for AD treatment work at different pathogenic stages and target either the acetylcholinesterase or Aβ [47]. Some drugs that are commercially marketed to block acetylcholinesterase are TACRIL, donepezil (Pfizer, NY), rivastigmine (Novartis), GALANTIME (Janssen,
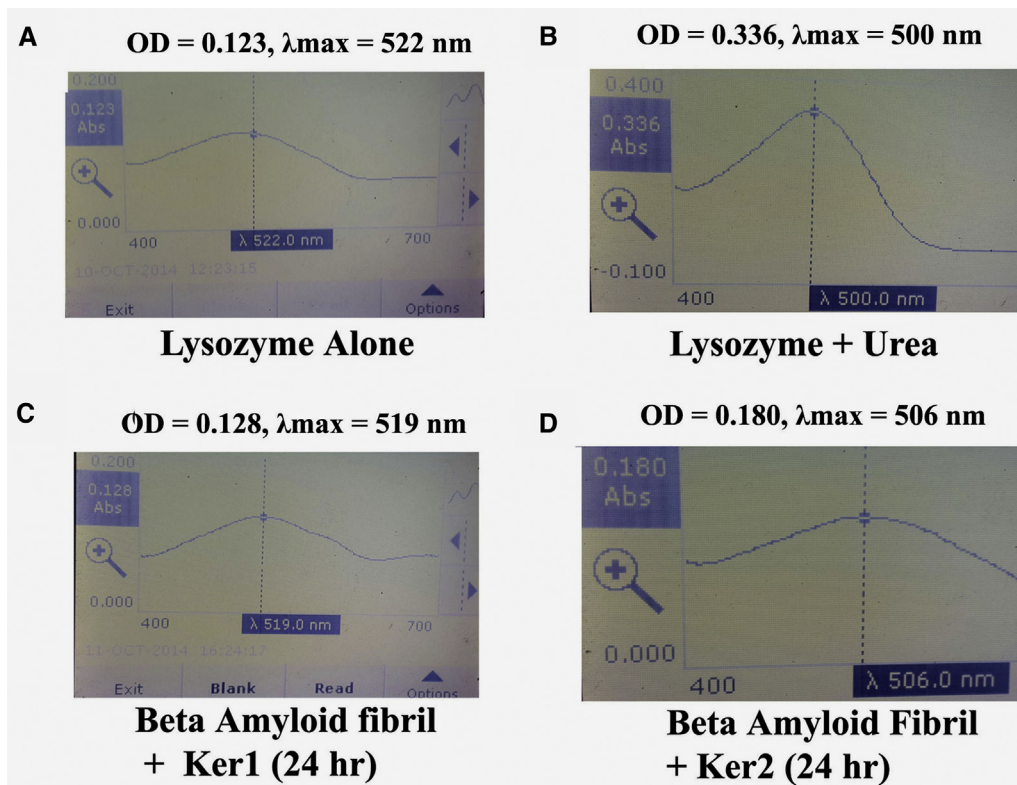
Fig. 5. Activity of Ker1 on β-amyloid (Aβ) fibrils revealed by Congo red absorption spectroscopy. The spectrum of Congo red is monitored in tubes containing: (A) Lysozyme alone (OD = 0.123, λ_{max} = 522 nm); (B) lysozyme treated with urea-forming Aβ fibrils (OD = 0.336, λ_{max} = 500 nm), hyperchromic, and blue shift of spectrum; (C) Aβ fibrils treated with Ker1, (OD = 0.128, λ_{max} = 519 nm), spectrum reverting back to a previous state; (D) Aβ fibrils treated with Ker2 for 24 hr (OD = 0.180, λ_{max} = 506 nm), hyperchromicity is reduced but blue shift of spectrum still exists. OD, optical density.

Belgium), and so forth. Although some of these drugs could improve cognitive performance, they suffer from various adverse health effects.

Aβ fibrils are major contributors to the progression and pathogenesis of AD, and their overproduction leads to synaptic dysfunction and formation of interneuronal fibrillary tangles and Aβ plaques. The Aβ plaques disrupt Ca^{++} channels, leading to loss in action potential of neurons leading to their denaturation. Antioxidants (selegiline and melatonin), Ca^{++} channel antagonists (nimodipine, flunarizine, verapamil, and tetrandrine), nonsteroidal anti-inflammatory drugs (indomethacin, tenidap, aspirin, ibuprofen, and naproxen), iron chelators, hypolipidemic drugs (desferrioxamine), and vaccination involving anti-Aβ antibodies target formation of Aβ or control its downstream adverse activities [48–50]. These drugs prevent Aβ fibrillogenesis and aggregation, inhibit Ca^{++} influx, inhibit inflammation, clears iron that cause neurotoxicity from brains, or clears Ac plaques. Some of these drugs are under clinical trials such as a new AD antibody, aducanumab, which degrades Aβ plaques and is ready to undergo phase III clinical trials. The drugs suffer from side effects such as hepatic and renal toxicity, injection-site reactions, retinal toxicity, subacute meningoencephalitis, as well as inability to globally benefit in cognition and behavior.

Microbial keratinases can be promising molecules to be tested for drug development in AD. Our results confirmed Ker1 effectively degrades Aβ fibrils of lysozyme *in vitro* within 24 hrs of incubation. Although keratinase has been purified almost 25 years back, its importance in treating prions is understood only recently. Aβs have cross β-pleated sheet structures similar to prions, and it was likely that keratinases could degrade Aβ fibrils also. However, no research groups have yet reported degradation of Aβ by keratinases. It can be due to lack of proper protocol for testing keratinases or due to lack of potent keratinases.

5. Next Steps

Ker1 activity can be tested on mouse models of AD. Various strategies attempt to overcome blood-brain barrier (BBB) and deliver drugs inside central nervous system for treating neurological diseases. Invasive methods involve direct delivery of drugs into brain tissues by polymer/microchip systems and so forth, whereas noninvasive strategy uses nanocarriers such as liposomes. Drugs in market/clinical trials for treating cryptococcal meningitis, pediatric tumors, and glioblastoma multiforme use nanocarrier strategy. As BBB consists of polyanions, our Ker1 docked liposomes (KD liposomes), being cationic, will bind electrostatically to BBB. However, for preclinical testing

on mice, we will PEGylate the KD liposomes, as PEGylation will improve biodistribution and pharmacokinetics of liposome in mouse brain. The PEGylated KD liposomes will be conjugated to anti-transferring antibody or holo-transferring *in vitro*. Intravenous injection of this formulation in mice will help in binding of antitransferrin antibody or holo-transferrin to the transferrin receptors in BBB endothelial cells, enabling KD liposomes to cross BBB, thereby delivering Ker1 inside mouse brains expressing Aβ plaques. We can monitor degradation of Aβ plaques by Ker1 *in vivo* by immunofluorescence staining of mouse brain tissue using anti-Aβ antibody. If successful preclinically, we will test the potentiality of KD liposomes for treatment of AD in clinical trials.

Acknowledgment

RESEARCH IN CONTEXT

1. Systematic review: We reviewed publications (including PubMed) searching for reports on amyloid digesting potential of microbial keratinases. Keratinases digesting prions have been reported; however, there is no report of any microbial keratinase-degrading β-amyloid (Aβ) fibrils. As prions and Aβ share similar cross β-pleated sheet-like structure, we purified microbial keratinases and screened for Aβ fibril degradation.

2. Interpretation: We purified two potent keratinases, Ker1 and Ker2, from an actinomycete *Amycolatopsis* sp. Ker1-digested Aβ fibrils *in vitro*. Ker2 was less potent. Both soluble Ker1 and Ker1 reconstituted on neutral/cationic liposomes had similar activities.

3. Future directions: We shall PEGylate our Ker1-loaded cationic liposomes for preclinical testing on mice as PEGylation improves biodistribution and pharmacokinetics of liposomes. Liposomes will be conjugated to antitransferrin antibody and administered through an intravenous formulation resulting in delivery of Ker1 inside the mouse brain. Activity of Ker1 in digesting Aβ fibrils can possibly be tested.

References

[1] Eanes ED, Glenner GG. X-ray diffraction studies on amyloid filaments. J Histochem Cytochem 1968;16:673–7.

[2] Glenner G, Ein D, Eanes ED, Bladen HA, Terry W, Page DL. Creation of "Amyloid" Fibrils from Bence Jones Proteins. Science 1971; 174:712–4.

[3] Sunde M, Serpell L, Bartlam M, Fraser PE, Pepys MB, Blake CC. Common core structure of amyloid fibrils by synchrotron X-ray diffraction. J Mol Biol 1997;273:729–39.

[4] Come JH, Fraser PE, T Lansbury JP. A kinetic model for amyloid formation in the prion diseases: importance of seeding. P Natl Acad Sci USA 1993;90:5959–63.

[5] Chiti F, Webster P, Taddei N, Clark A, Stefani M, Ramponi G, et al. Designing condi-tions for in vitro formation of amyloid protofilaments and fibrils. Biochemistry 1999;96:3590–4.

[6] DerSarkissian A, Jao CC, Chen J, Langen R. Structural organisation of alpha-synuclein studied by site-directed spin labelling. J Biol Chem 2003;278:37530–5.

[7] Jayasinghe SA, Langen R. Identifying structural features of fibrillar islet amyloid polypeptide using site-directed spin labeling. J Biol Chem 2004;279:48420–5.

[8] Torok M, Milton S, Kayed R, Wu P, McIntire T, Glabe CG, et al. Structural and dynamic features of Alzheimer's Abeta peptide in amyloid fibrils studied by site-directed spin labelling. J Biol Chem 2002;277:40810–5.

[9] Divry P, Florkin M. Sur les proprietes optiques de l'amyloid. Societe de Biologie 1927;97:180–1.

[10] Irvine GB, El-Agnaf OM, Shankar GM, Walsh DM. Protein aggregation in the brain: the molecular basis for Alzheimer's and Parkinson's diseases. Mol Med 2008;14:451–64.

[11] Morris AM, Watzky MA, Finke RG. Protein aggregation kinetics, mechanism, and curve-fitting: a review of the literature. Biochim Biophys Acta 2009;1794:375–97.

[12] Ross CA, Poirier MA. Protein aggregation and neurodegenerative disease. Nat Med 2004;10:S10–7.

[13] Uversky VN. Mysterious oligomerization of the amyloidogenic proteins. FEBS J 2010;277:2940–53.

[14] Serpell LC. Alzheimer's amyloid ¢brils: structure and assembly. Biochim Biophys Acta 2000;1502:16–30.

[15] Prusiner SB, Scott MR, DeArmond SJ, Cohen FE. Prion protein biology. Cell 1998;93:337–48.

[16] Weissmann C. Molecular genetics of transmissible spongiform encephalopathies. J Biol Chem 1999;274:3–6.

[17] Ernst DR, Race RE. Comparative analysis of scrapie agent inactivation methods. J Virol Methods 1993;41:193–201.

[18] Taylar DM. Transmissible degenerative encephalopathies, inactivation of the causal agents. In: Russel AD, Hugo WB, Anyliffe GAJ, eds. Principles and Practice of Disinfection Preservation and Sterilization. Oxford: Blackwell Scientific Publications; 1992. p. 171–9.

[19] Gibbs CJ Jr, Gajdusek DC, Latarjet R. Unusual resistance to ionizing radiation of the viruses of kuru, Creutzfeldt-Jakob disease, and scrapie. Proc Natl.Acad Sci USA 1978;75:6268–70.

[20] Onifade AA, Al-Sane NA, Al-Musallam AA, Al-Zarban S. A review: potentials for biotechnological applications of keratin-degrading microorganisms and their enzymes for nutritional improvement of feathers and other keratins as livestock feed resources. Bioresour Technology 1998;66:1–11.

[21] Bahuguna S, Kushwaha RKS. Hair perforation by keratinophilic fungi. Mycoses 1989;32:340–3.

[22] Kushwaha RKS, Gupta P. Relevance of keratinophilic fungi. Cur Sci 2008;94:706–7.

[23] Mitsuiki S, Takasugi M, Moriyama Y, Futagami T, Golo M, Kanouchi H, et al. Identification of alkaliphilic actinomycetes that produces a PrPSc degrading enzyme. Am Microbiol 2010;60:349–53.

[24] Korkmaz H, N Unaldi M, Aslan B, Coral G, Arikan B, Dincer S, et al. Keratinolytic activity of *Streptomyces* strain BA7, a new isolate from Turkey. Ann Microbiol 2003;53:85–93.

[25] Gong JS, Wang Y, Zhang DD, Zhang RX, Su C, Li H, et al. Biochemical characterization of an extreme alkaline and surfactant-stable keratinase derived from a newly isolated actinomycete *Streptomyces aureofaciens* K13. RSC Adv 2015;5:24691–9.

[26] Williams CM, Ritcher CS, MacKenzie JM Jr, H Shih JC, Isolation. identification and characterization of feather-degrading bacterium. Appl Environ Microbiol 1990;56:1509–15.

[27] Gupta R, Ramnani P. Microbial keratinases and their prospective applications: an overview. Appl Microbiol Biotech 2005;70:21–33.

[28] Kublanov IV, Perevalova AA, Slobodkina GB, Lebedinsky AV, Bidzhieva SK, Kolganova TV, et al. Biodiversity of thermophilic prokaryotes with hydrolytic activities in hot springs of Uzon Caldera, Kamchatka (Russia). Appl Environ Microb 2009;75:286–91.

[29] Lin X, Lee CG, Casale ES, Shih JCH. Purification and characterization of a keratinase from a feather degrading *Bacillus licheniformis* strain. Appl Environ Microb 1992;58:3271–5.

[30] Muller-Hellwig S, Groschup MH, Pichner R, Gareis M, Martlbauer E, Scherer S, et al. Biochemical evidence for the proteolytic degradation of infectious prion protein prpSc in hamster brain homogenates by foodborne bacteria. Syst Appl Microbiol 2006;29:165–71.

[31] Yoshioka M, Miwa T, Horii H, Takata M, Yokoyama T, Watanabe KNishizawa M, et al. Characterization of a proteolytic enzyme derived from a *Bacillus* strain that effectively degrades prion protein. J Appl Microbiol 2007;102:509–15.

[32] Dickinson AG, Outram GW. The scrapie replication-site hypothesis and its implications for pathogenesis. In: Prusiner SB, Hadlow WJ, eds. Slow Transmissible Diseases of the Nervous System. New York: Academic Press; 1979. p. 13–31.

[33] Liang X, Bian Y, Tang X-F, Xiao G, Tang B. Enhancement of keratinolytic activity of a thermophilic subtilase by improving autolytic resistance and thermostability under reducing conditions. Appl Microbiol Biotechnol 2010;87:999–1006.

[34] Ningthoujam DS, Jaya Devi L, Jolly Devi P, Kshetri1 P, Tamreihao K, Mukherjee S, et al. Optimization of Keratinase Production by Amycolatopsis sp. Strain MBRL 40 from a Limestone Habitat. J Bioprocessing Biotechniques 2016;6.

[35] Dobson CM. Protein misfolding, evolution and disease. Trends Biochem Sci 1999;24:329–32.

[36] Fandrich M, Fletcher MA, Dobson CM. Amyloid fibrils from muscle myoglobin. Nature 2001;410:165–6.

[37] Bucciantini M, Giannoni E, Chiti F, Baroni F, Formigli L, Zurdo J, et al. Inherent toxicity of aggregates implies a common mechanism for protein misfolding disease. Nature 2002;416:507–11.

[38] Lansbury PT. Evolution of amyloid: What normal protein folding may tell us about fibrillogenesis and disease. Proc Natl Acad Sci 1999; 96:3342–4.

[39] R Krebs M, Wilkins DK, Chung EW, Pitkeathly MC, Chamberlain AK, Zurdo J, et al. Formation and seeding of amyloid fibrils from wild-type hen lysozyme and a peptide fragment from the domain. J Mol Biol 2000;300:541–9.

[40] Arnaudov LN, de Vries R. Thermally induced fibrillar aggregation of hen egg white lysozyme. Biophysical J 2005;88:515–26.

[41] Goda S, Takano K, Yamagata YR, Nagata R, Akutsu H, Maki S, et al. Amyloid protofilament formation of hen egg lysozyme in highly concentrated ethanol solution. Protein Sci 2000;9:369–75.

[42] Vernaglia BA, Huang J, Clark ED. Guanidine hydrochloride can induce amyloid fibril formation from hen egg-white lysozyme. Biomacromolecules 2004:1362–70.

[43] Bockle B, Galunsky B, Muller R. Characterization of a keratinolytic serine proteinase from *Streptomyces pactum* DSM 40530. Appl Environ Microbiol 1995;61:3705–10.

[44] Ramnani P, Singh R, Gupta R. Keratinolytic potential of Bacillus licheniformis RG1: structural and biochemical mechanisms of feather degradation. Can J Microbiol 2005;51:191–6.

[45] Kunitz M. Crystalline Soybean Trypsin Inhibitor: II General Properties. J Gen Physiol 1947;30:291–310.

[46] Relini A, Cavallari O, Canale C, Svaldo Lanero T. What can Atomic Force Microscopy say about Amyloid aggreagrates? In: Bhusan Bharat, Fuchs Harald, Tomitori Masahiko, eds. Applied Scanning Probe Methods IX: Characterization. Springer; 2008. p. 182–4. ISBN 978-3-540-74083.

[47] Xiaoting S, Lan J, Peixue L. Review of drugs for Alzheimer's disease. Drug Discoveries Ther 2012;6:285–90.

[48] He H, Dong W, Huang F. Anti-amyloidogenic and antiapoptotic role of melatonin in Alzheimer disease. Curr Neuropharmacol 2010; 8:211–7.

[49] L Krause D, Muller N. Neuroinflammation, microglia and implications for anti-inflammatory treatment in Alzheimer's disease. Int J Alzheimers Dis 2010;10:1–9.

[50] N Xing X, Zhang WG, Sha S, Li Y, Guo R, Wang C, et al. Amyloid β3-10 DNA vaccination suggests a potential new treatment for Alzheimer's disease in BALB/c mice. Chin Med J 2011;124:2636–41.